Uncertainty Propagation and Analysis of Image-guided Surgery

Amber L. Simpson[a], Burton Ma[b], Randy E. Ellis[c], A. James Stewart[c], and Michael I. Miga[a]

[a] Department of Biomedical Engineering, Vanderbilt University, Nashville, Tennessee, USA
[b] Department of Computer Science and Engineering, York University, Toronto, Ontario, Canada
[c] School of Computing, Queen's University, Kingston, Ontario, Canada

ABSTRACT

A successful image-guided surgical intervention requires accurate measurement of coordinate systems. Uncertainty is introduced every time a pose is measured by the optical tracking system. When we transform a measured pose into a different coordinate system, the covariance (which encodes the uncertainty of the pose) must be propagated to this new coordinate system. In this paper, we describe a method for propagating covariances estimated from registration, tracking, and instrument calibration into the tip of the surgical tool. This is clinically important, since it is at the tool tip that the clinician cares about uncertainty. We demonstrate that the propagation method, which is computed in real time as the tool moves through space, reliably computes the propagated covariance by comparing our estimate to true covariances from Monte Carlo simulations.

Keywords: uncertainty, surgical navigation, image guidance, accuracy, error analysis

1. INTRODUCTION

The introduction of error in image-guided surgery in inevitable. It cannot be avoided by simply taking very careful measurements, providing more accurate algorithms, or by improving instrument calibration. We can only reduce errors as much as reasonably possible, calculate a reliable estimate of the uncertainty, and provide a meaningful way to convey this information to clinicians.

The success of an image-guided surgical intervention is contingent on the accurate measurement of coordinate systems. Uncertainty is introduced each time data is introduced from an optical tracking system. When we transform a pose into a different coordinate system, the covariance (uncertainty) must be propagated to this new frame of reference. The measurement of coordinate systems by optically tracked instruments has both rotational and translational errors. The effect of orientation error on positional error has been studied and can, in some cases, be dramatic.[1–3]

This paper describes a method of propagating covariances from registration, calibration, and tracking and studies the effect of this propagation at the tip of the surgical instrument. The accuracy of the uncertainty propagation is validated using the heteroscedastic errors in variables (HEIV) algorithm.[4] Our simulations show that the propagation method reliably estimates covariance under the assumed noise conditions. Once the covariance propagation is known, we can then study the key factors influencing the uncertainty. We can ask questions regarding the important contributors for further analysis and determine the tails in our distributions. In this paper, we focus on uncertainty propagation, rather than on an analysis of the covariances.

2. BACKGROUND

Surgical navigation systems rely on optical tracking technology for determining the pose (position and orientation) of instruments relative to some coordinate frame. Using the notation and description from Hoff and Vincent[5] and Craig,[6] we can represent the pose of a rigid body {A} with respect to a coordinate frame {B} with a six element vector $\mathbf{x}_A^B = [x_{A_{org}}^B, y_{A_{org}}^B, z_{A_{org}}^B, \alpha, \beta, \gamma]^T$ where $\mathbf{p} = x_{A_{org}}^B, y_{A_{org}}^B, z_{A_{org}}^B$ is the origin of frame {A} in {B} and α, β, γ the angle of rotation of {A} about the z, y, x axes of {B}. Pose can be represented in the equivalent matrix operator form with a 4×4 homogeneous transformation matrix:

$$\mathbf{T}_A^B = \begin{pmatrix} \mathbf{R}_A^B & \mathbf{p}_{A_{ORG}}^B \\ 0 & 1 \end{pmatrix} \tag{1}$$

---

where $\mathbf{R}_A^B$ is the 3×3 rotation matrix corresponding to the angles α, β, γ. In this paper, we will use the letter $\mathbf{T}$ to designate the equivalent 4×4 homogeneous transformation matrix. The homogenous matrix represented the pose of coordinate frame {B} with respect to {A} is the inverse of the pose of {A} with respect to {B}: $\mathbf{T}_B^A = (\mathbf{T}_A^B)^{-1}$. If we know the pose of {A} with respect to {B} and the pose of {B} with respect to {C} then the pose of {A} with respect to {C} is given by $\mathbf{T}_A^C = \mathbf{T}_B^C \mathbf{T}_A^B$.[6]

If we have a pose of a rigid body, we can represent the uncertainty of the six-element pose $\mathbf{x}$ with a 6×6 covariance matrix $\mathbf{C_x} = E(\mathbf{\Delta x \Delta x}^T)$, the expected value of the square of the difference between the estimate and the ground truth.[5]

Our work assumes that a reliable covariance of a rigid transformation is available. Finding the rigid transformation that best matches one point to set to another where the point correspondences are known is called the fiducial registration problem in computer-aided surgery literature. Estimating the covariance matrix of fiducial registration parameters has been studied. Matei and Meer describe an algorithm that produced optimal estimates of rotation and translation with confidence intervals obtained from bootstrapping.[4] Ma et al.[7,8] described a particle filter that estimated the covariance of surface-based registration parameters, Moghari and Abolmaesumi[2] used the unscented Kalman filter to estimate the covariance of target registration error (TRE). More recently, Ma et al.[1] derived an analytic expression for predicting TRE. Danilchenko and Fitzpatrick[9] determined cross covariances for TRE and FRE.

3. METHODS

We assume that an optical tracking system measures the pose of a target relative to the tracker's coordinate system, which we call the "world" coordinate system. A target attached to the surgical tool has pose $\mathbf{p}_{tool}$ (in world coordinates) which is encoded as a tracking transformation $\mathbf{T}_{tool}^{world}$. Another target attached to the patient has pose $\mathbf{p}_{patient}$ (in world coordinates) which is encoded as a tracking transformation $\mathbf{T}_{patient}^{world}$.

The calibration transformation $\mathbf{T}_{tip}^{tool}$ maps the tool tip coordinates (typically with the origin at the tool tip) to tool coordinates and is the result of a calibration procedure. The registration transformation $\mathbf{T}_{patient}^{CT}$ maps patient coordinates to CT coordinates and is the result of a registration procedure.

The surgeon's guidance display shows the CT and the tracked tool in CT coordinates. So we must transform the tool tip into CT coordinates, as follows:

$$\mathbf{T}_{tip}^{CT} = \mathbf{T}_{patient}^{CT} \, (\mathbf{T}_{patient}^{world})^{-1} \, \mathbf{T}_{tool}^{world} \, \mathbf{T}_{tip}^{tool}. \tag{2}$$

3.1 Covariance Propagation

Each of the transformations, $\mathbf{T}_x^y$, in Equation (2) has an associated covariance matrix, $\mathbf{C}_x^y$, that encodes the uncertainty in the transformation. The eigenvectors and eigenvalues of the covariance matrix show the principal directions of uncertainty and the magnitudes of the uncertainty in those directions. The uncertainty can arise from tracking error ($\mathbf{C}_{tool}^{world}$ and $\mathbf{C}_{patient}^{world}$), from calibration error ($\mathbf{C}_{tip}^{tool}$), and from registration error ($\mathbf{C}_{patient}^{CT}$).

We want to display to the surgeon the uncertainty of the pose of the tool tip, so we must determine the uncertainty of the tool tip pose in CT coordinates. That uncertainty, encoded by the covariance matrix $\mathbf{C}_{tip}^{CT}$, is computed from the covariances of the transformations on the right hand side of Equation (2).

The covariances are propagated through the chain of transformations in Equation (2) using a method described by Hoff and Vincent,[5] which they used to propagate head pose covariance in virtual reality systems. The following description is drawn from Hoff and Vincent's paper;[5] the reader is directed to the original source for more detailed treatment of the subject.

Given a transformation $\mathbf{y} = \mathbf{T_w x}$, let $\mathbf{C_x}$ be the covariance of $\mathbf{x}$ and let $\mathbf{C_w}$ be the covariance of $\mathbf{T_w}$. Then the covariance $\mathbf{C_y}$ of $\mathbf{y}$ is computed as

$$\mathbf{C_y} = \mathbf{J_x C_x J_x}^T + \mathbf{J_w C_w J_w}^T \tag{3}$$

where $\mathbf{J_x} = \partial \mathbf{g}/\partial \mathbf{x}$ and $\mathbf{J_w} = \partial \mathbf{g}/\partial \mathbf{w}$, for $\mathbf{g}(\mathbf{w}, \mathbf{x}) = \mathbf{T_w x}$. If the transformation $\mathbf{T_w}$ has no uncertainty, the covariance $\mathbf{C_w}$ is zero and Equation (3) is simplified.

Thus, given the covariances associated with each transformation on the right hand side of Equation (2), we can compute the uncertainty, encoded as $\mathbf{C}_{tip}^{CT}$, of the tool tip pose. In our implementation, the Jacobian matrices were estimated numerically.

3.2 Simulations

We validated this method of covariance propagation through Monte Carlo simulation of a virtual patient and a virtual tool. In that simulation, calibration uncertainty ($\mathbf{C}_{tip}^{tool}$), tool tracking uncertainty ($\mathbf{C}_{tool}^{world}$), and patient tracking uncertainty ($\mathbf{C}_{patient}^{world}$) were estimated using an unscented Kalman filter method described in other work.[10] An estimate of registration uncertainty ($\mathbf{C}_{patient}^{CT}$) was computed based on neurosurgical patient data collected at Vanderbilt University Medical Center. The registration uncertainty was computed as follows. Preoperatively, skin fiducials were placed on the patient's skull and the patient underwent an MR. These fiducials are visible in the MR. Intraoperatively, points were taken on the head of the patient by touching a calibrated tool to skin fiducials (see Figure 1). A registration of the collected points to the MR patient space establishes correspondence. The registration covariance ($\mathbf{C}_{patient}^{CT}$) was computed based on 10,000 HEIV estimates of Matei and Meer,[4] which optimally solves the absolute orientation problem under the assumption of heteroscedastic noise.

Figure 1. An optically-tracked calibrated tool collecting registration from skin fiducials from a patient undergoing a neurosurgical procedure at Vanderbilt University Medical Center.

In each simulated trial, the pose of the patient target remained fixed and the tool target was rotated about its center by applying uniformly sampled rotations from $-50°$ to $50°$ at $10°$ increments about the x axis and successive rotations drawn in the same way about the y axis. For each such pose, we computed the covariance and propagated it through the chain of transformations of Equation (2). The resulting tool tip covariance, $\mathbf{C}_{tip}^{CT}$, was compared to a gold standard covariance computed using 10,000 estimates from the HEIV algorithm,[4] which produces an optimal estimate of rotation and translation under heteroscedastic noise.

The HEIV algorithm uses a model of the virtual tracking targets on the patient and on the tool to compute the $\mathbf{T}_{patient}^{world}$ and $\mathbf{T}_{tool}^{world}$ transformations. Our virtual targets consisted of four LED markers in a quadrilateral configuration. The marker

coordinates were $[0 -50\ 0]^T$, $[-50\ 0\ 0]^T$, $[0\ 50\ 0]^T$, and $[50\ 0\ 0]^T$ in millimeters in the tool coordinate system. The tip of the surgical tool was defined as $[0\ 0 -200]^T$ in the tool coordinates. The camera and tool models are shown in Figure 2.
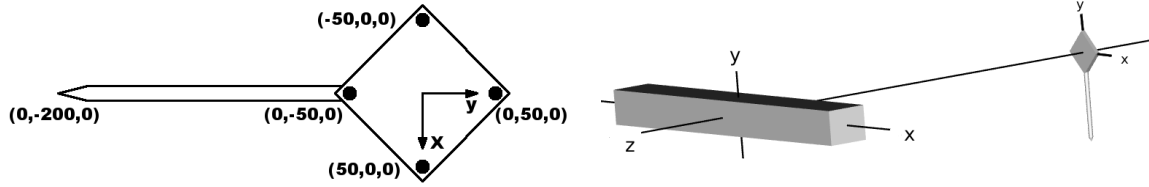

Figure 2. Target model (left) and optical tracking system configuration (right) used in the simulations; all units are in millimeters. The target consisted of four markers arranged in a quadrilateral. Measurement noise in the viewing direction, –z, was larger than in the viewing plane. The patient target was oriented to face the camera, as shown in the figure.

4. RESULTS

In the first simulation, the calibration covariance in the tip of the tool, $\mathbf{C}_{tip}^{tool}$, and the registration covariance, $\mathbf{C}_{patient}^{CT}$, were set to zero. Figure 3 plots the difference between the covariances measured by our model and those of the gold standard HEIV algorithm. In the figure, the square root of the eigenvalues of the covariances are plotted for each angle of rotation applied in the simulation. The propagated covariances are shown in Figure 4.

Figure 5 shows the effect on the tip of the tool when a nonzero calibration covariance is incorporated into the model. In this example, the calibration covariance, $\mathbf{C}_{tip}^{tool}$, was drawn from a previous study of calibration uncertainty,[10] where the calibration covariance had eigenvalues with square roots $[0.31\ 0.40\ 0.91]^T$ in the position of the tip of the surgical tool (in millimeters).

Figure 6 shows the effect on the tip of the tool when calibration covariance and registration covariance are nonzero. This example uses registration covariance computed based on data acquired during a neurosurgical intervention as described in the previous section. In this example, the registration covariance had eigenvalues with square roots $[0.25\ 0.91\ 1.27]^T$ for position (in millimeters) and square roots $[0.00\ 0.00\ 0.10]^T$ for orientation (in degrees).

Figure 7 depicts a visualization of the covariance on the tip of the surgical tool. The surgical tool is rendered in cyan. The covariance is applied to the pose of the tool using a method described in other work[10] and rendered in magenta lines. The spread of the lines corresponds to approximately the 95th confidence interval.
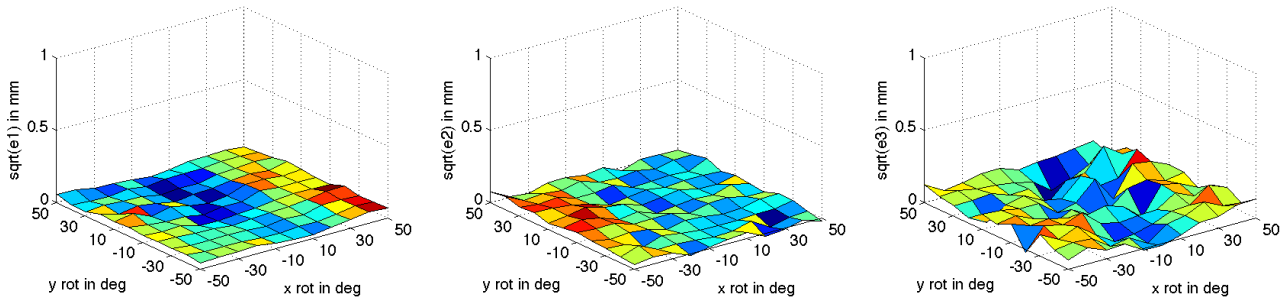

Figure 3. The differences in the covariance of the tip position x (left), y (center), z (right) measured by our model and the gold standard covariance computed from 10,000 HEIV simulations. The square roots of the eigenvalues of the covariance matrix are shown for rotations from $-50°$ to $50°$ at $10°$ increments about X and Y.

5. DISCUSSION

The covariance propagation model computes estimates of uncertainty in real time. In other work,[10] we used the model while actively navigating with the tool with no discernible lag in the display.
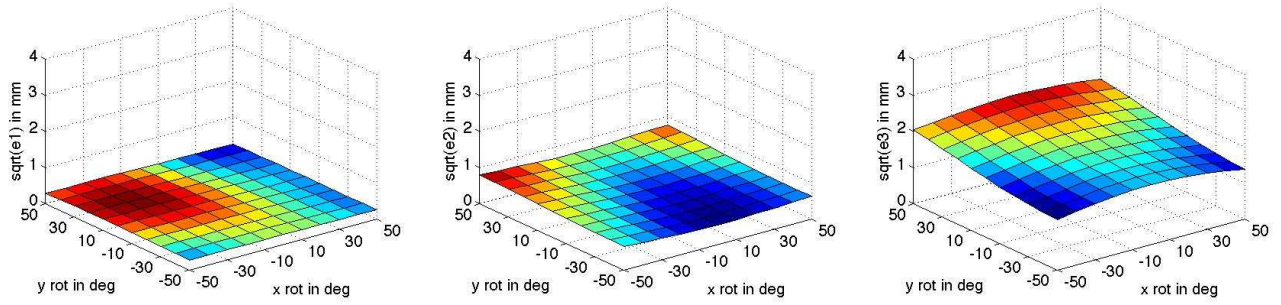
Figure 4. Covariances $\mathbf{C}_{tip}^{CT}$ predicted by our model, with zeroed registration covariance and zeroed calibration covariance, for tip position x (left), y (center), z (right). Square roots of the eigenvalues of the covariance matrix are shown for rotations from $-50°$ to $50°$ at $10°$ increments about X and Y.
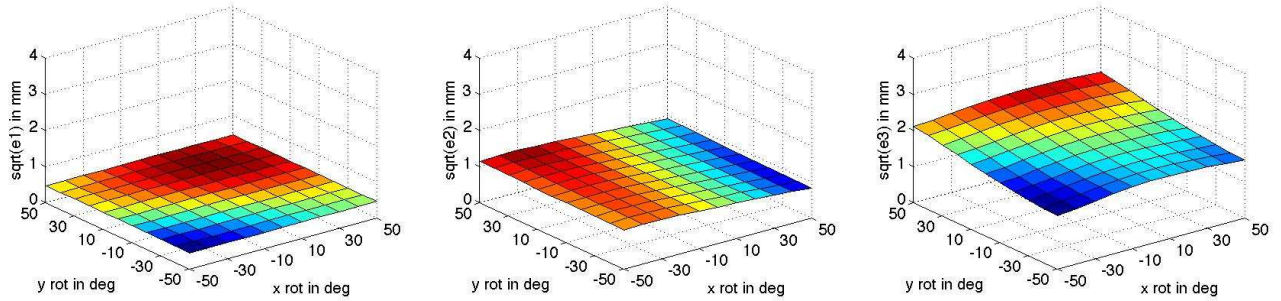

Figure 5. Covariances $\mathbf{C}_{tip}^{CT}$ predicted by our model, with zeroed registration covariance where the calibration covariance had eigenvalues with square roots $[0.31\ 0.40\ 0.91]^{\mathrm{T}}$ for tip position x (left), y (center), z (right). Square roots of the eigenvalues of the covariance matrix are shown for rotations from $-50°$ to $50°$ at $10°$ increments about X and Y.
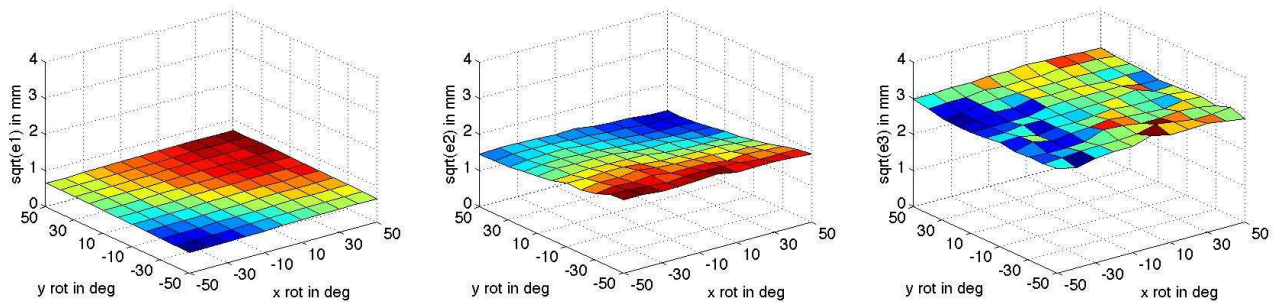

Figure 6. Covariances $\mathbf{C}_{tip}^{CT}$ predicted by our model, with registration covariance and calibration covariance, for tip position x (left), y (center), z (right). Square roots of the eigenvalues of the covariance matrix are shown for rotations from $-50°$ to $50°$ at $10°$ increments about X and Y.
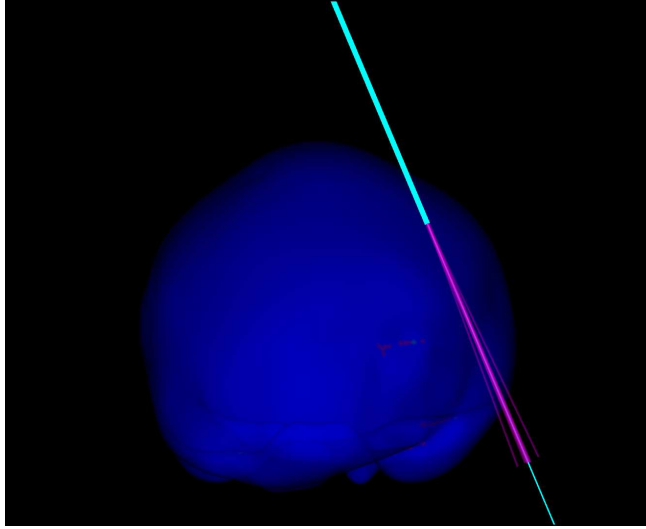
Figure 7. A visualization of the uncertainty in the tip of the surgical tool $\mathbf{C}_{tip}^{CT}$ predicted by our model based on data acquired intraoperatively. The thicker cyan tube corresponds to the tool, the thinner cyan tube is the path of the tool, and the magenta lines represent the uncertainty. The spread of the magenta lines corresponds to approximately the 95th confidence interval.

The values that we chose for registration covariance were derived from patient data; hence, the propagated covariances are indicative of what we would expect to encounter in the operating room. These values were based on point-based registration from fiducials; the registration was not refined using, for example, features from the cortical surface. Hence, the propagated covariances presented here do not consider the effect of brain shift that occurs during neurosurgical procedures which is known to have a significant effect on accuracy.[11] Furthermore, the registration covariance that we chose had very little rotational uncertainty. The purpose of the paper was to show that we could propagate the covariances, not to address the potential magnitude of uncertainty.

For simplicity, we computed actual registration covariances based on 10,000 registration estimates rather than using a TRE estimator.[1–3] Ideally, the registration algorithm would compute a reliable covariance of the registration parameters internally. Moreover, our registration covariance did not take into account the uncertainty in the tracked tool that acquired the registration points.

6. CONCLUSIONS

We proposed and validated a covariance propagation technique that can be used at interactive rates in the operating room. We demonstrated that our covariance estimates match well with gold standard covariances computed using the HEIV algorithm. The next step in this research is to formalize the analysis of the uncertainty and to determine the greatest contributors of uncertainty.

A crucial step in error and uncertainty analysis is the meaningful conveyance of uncertainty to clinicians. The visualization of uncertainty is absent from current commercial computer-assisted surgery systems. In fact, the only error information (if any) given to surgeons is a scalar value representing registration error. Anatomical data is presented to the surgeon as though it were perfect. A surgeon who is not aware of this uncertainty can make critical errors (consider, for example, excising a brain tumor or inserting a screw into the spine).

7. ACKNOWLEDGMENTS

REFERENCES

[1] Ma, B., Moghari, M. H., Ellis, R. E., and Abolmaesumi, P., "Estimation of optimal fiducial target registration error in the presence of heteroscedastic noise," *IEEE Transactions on Medical Imaging* **29**, 708–723 (2010).

[2] Moghari, M. H. and Abolmaesumi, P., "Distribution of fiducial registration error in rigid-body point-based registration," *IEEE Transactions on Medical Imaging* **28**, 1791–1801 (2009).

[3] Wiles, A. D., Likholyot, A., Frantz, D. D., and Peters, T., "A statistical model for point-based target registration error with anisotropic fiducial localizer error," *IEEE Transactions on Medical Imaging* **27**, 378–390 (2008).

[4] Matei, B. and Meer, P., "Optimal rigid motion estimation and performance evaluation with bootstrap," in [*IEEE Conference on Computer Vision and Pattern Recognition*], 339–345 (1999).

[5] Hoff, W. and Vincent, T., "Analysis of head pose accuracy in augmented reality," *IEEE Transactions on Visualization and Computer Graphics* **6**, 319–334 (2000).

[6] Craig, J. J., [*Introduction to Robotics: Mechanics and Control*], Prentice Hall, 3rd ed. (2005).

[7] Ma, B. and Ellis, R. E., "Surface-based registration with a particle filter," in [*MICCAI 2007, LNCS Vol. 3216*], Barillot, C., Haynor, D., and Hellier, P., eds., 566–573, Springer (2004).

[8] Ma, B., Moghari, M. H., Ellis, R. E., and Abolmaesumi, P., "On fiducial target registration error in the presence of anisotropic noise," in [*MICCAI 2007, LNCS Vol. 4792*], Ayache, N., Ourselin, S., and Maeder, A., eds., 628–635, Springer–Verlag, Berlin (2007).

[9] Danilchenko, A. and Fitzpatrick, J., "General approach to error prediction in point registration," in [*SPIE Medical Imaging 2010, Vol:7625*], 14 (2010).

[10] Simpson, A. L., *The Computation and Visualization of Uncertainty in Surgical Navigation*, PhD thesis, School of Computing, Queen's University (2010).

[11] Dumpuri, P., Thompson, R. C., Dawant, B. M., Cao, A., and Miga, M. I., "An atlas-based method to compensate for brain shift: Preliminary results," *Medical Image Analysis* **11**, 128–45 (2007).